

Rapid Communications

The Rapid Communications section is intended for the accelerated publication of important new results. Since manuscripts submitted to this section are given priority treatment both in the editorial office and in production, authors should explain in their submittal letter why the work justifies this special handling. A Rapid Communication should be no longer than 3½ printed pages and must be accompanied by an abstract. Page proofs are sent to authors, but, because of the accelerated schedule, publication is not delayed for receipt of corrections unless requested by the author or noted by the editor.

Generation of microwave radiation in the tunneling junction of a scanning tunneling microscope

W. Krieger, T. Suzuki,* and M. Völcker

Max-Planck-Institut für Quantenoptik, D-8046 Garching, Federal Republic of Germany

H. Walther

Max-Planck-Institut für Quantenoptik and Sektion Physik der Universität München,

D-8046 Garching, Federal Republic of Germany

(Received 20 February 1990)

Difference-frequency generation at 9 GHz and laser-light rectification was demonstrated in the tunneling junction of a scanning tunneling microscope (STM) using CO₂ laser radiation. Simultaneous measurements of mixing signals and the current-voltage (*I-V*) characteristics of the STM show that the mixing process occurs at the nonlinearity of the static *I-V* curve.

I. INTRODUCTION

A combination of laser excitation and scanning tunneling microscopy can result in a powerful method of identifying and locating surface adsorbates. For the development of this spectroscopy it is important to study the interaction of laser radiation with the tunneling junction of the scanning tunneling microscope (STM).

The interaction of electromagnetic radiation with a similar nonlinear device, the point-contact metal-insulator-metal (MIM) diode, has been extensively investigated.¹ The MIM diode is used to generate harmonics and difference frequencies of injected microwave and laser radiation for precision frequency measurement of laser light. The tunneling junction of both devices, the MIM diode and the STM, usually consists of a fine metal tip and a conducting substrate separated by a very thin insulating layer. The insulator is an oxide in the MIM diode and a vacuum gap in the STM. The essential properties of both junctions relevant to interaction with electromagnetic radiation are their nonlinear current-voltage characteristic and their extremely small response time, which is limited by the tunneling time of the electrons and the *RC* time constant of the junction.

The vacuum gap of the STM, however, is inherently simpler than an oxide gap. Its width is precisely controllable by adjusting the tunneling current, and only a few atoms are involved in the tunneling process. The study of frequency mixing and rectification of electromagnetic radiation in the STM will, therefore, also shed light on the physical mechanisms responsible for these processes in the MIM diode, which are still not sufficiently understood, and it may establish the STM as a frequency mixing de-

vice of higher efficiency and better stability.

First experiments using the STM for the generation of difference frequency signals up to 100 MHz have already been reported.²⁻⁴ The radiation of two CO₂ lasers was focused into the tunneling junction of the STM, and the mixing signals were directly taken from the tip or the sample. Generation of harmonics of the difference frequency and mixing with radio-frequency signals were also observed.^{3,4} An experiment using the nonlinearity of the tunneling junction for laser-light rectification and its application for measuring the tunneling time of the electrons was proposed.⁵ Meanwhile, preliminary results have been published.⁶

Here we report experiments where the STM is used for infrared laser frequency mixing at far higher difference frequencies of 5 and 9 GHz. In addition laser-light rectification was observed. The experimental results show that the static current-voltage characteristic of the tunneling junction can be used to describe the mixing process at difference frequencies in the GHz range.

II. EXPERIMENT

The experimental setup consists of the STM, two tunable CO₂ lasers, and the microwave circuit for detecting the mixing signal emitted by the tip. The STM used for the experiments has already been described in detail.³ The surface sample chosen was highly oriented pyrolytic graphite which was freshly cleaved before each measurement. The experiments were carried out at ambient air pressure. The STM was used without lateral scan.

The two CO₂ lasers were filled with different CO₂ iso-

topes in order to increase the range of selectable difference frequencies. For the present experiments difference frequencies of $\Delta\nu=5$ and 9 GHz were provided by tuning the lasers to different transitions in the (001-020) branch close to $9.3\ \mu\text{m}$ [$P(16)$ of $^{12}\text{C}^{18}\text{O}_2$ and $R(10)$ of $^{12}\text{C}^{16}\text{O}_2$ for $\Delta\nu=5$ GHz, and $P(14)$ of $^{12}\text{C}^{18}\text{O}_2$ and $R(12)$ of $^{12}\text{C}^{16}\text{O}_2$ for $\Delta\nu=9$ GHz]. The two beams were combined at a beam splitter, suitably attenuated, and focused into the tunneling junction of the STM with a ZnSe lens of 38-mm focal length. The focal-spot diameter was about $60\ \mu\text{m}$.

To optimize the mixing signal, the angle between the incident laser beam and the tip axis was set at 30° , and the polarization direction was rotated into the plane defined by the laser beam and the tip. At perpendicular polarization the mixing signal was reduced by about 15 dB. In addition it was found that the signal decreased for increasing cone angle of the tungsten tips. For most of the tips this angle was close to 15° . From tip to tip the mixing signal differed by as much as 30 dB. These results are explained by assuming that the front end of the tip, which has a smaller diameter than the laser wavelength, represents a long-wire antenna for the incident laser radiation.

The tip also acts as a transmission antenna for the difference-frequency signal which is generated in the tunneling junction. Part of this radiation was collected by a pyramidal microwave horn mounted directly above the STM. The signal was amplified by 84 dB by means of two low-noise narrow-band amplifiers and detected with a spectrum analyzer.

III. RESULTS

We observed difference-frequency generation at 5 and 9 GHz, using a total laser power as small as a few mW. The radiated mixing signals were strongly polarized in the direction of the tip, as was found by rotating the microwave horn. For $\Delta\nu=5$ GHz also the second-harmonic signal at 10 GHz was detected with a signal level reduced by 40 dB.

The measurements described below were done at a difference frequency of 9 GHz. At an input power of 100 mW, signals as large as 1 nW were measured at the microwave horn. A considerably lower mixing efficiency was observed in a similar experiment where the laser radiation of two pulsed CO_2 lasers was mixed in a MIM diode to give a difference frequency of 54 GHz.⁷

A more detailed characterization of the STM junction as a frequency mixer was obtained by simultaneously measuring the current-voltage characteristic and the bias dependence of the mixing signal. For these experiments the STM was controlled by a computer which generated a bias voltage ramp with a length of 1 s, interrupted the current feedback during the voltage scans, and stored the measured data. Between the scans the tip-sample distance was reset to a constant value by applying a fixed bias voltage and maintaining a constant tunneling current.

Mixing signals and the corresponding current-voltage characteristics are presented in Figs. 1(a) and 2(a). The curves are averages over ten single measurements. The single measurements differ from the averaged curves by

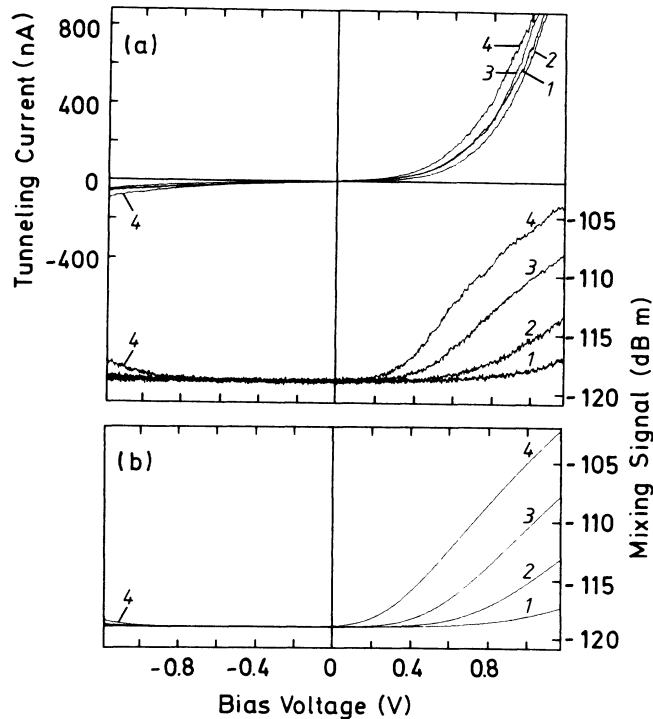


FIG. 1. (a) Plot of the tunneling current (upper part) and the mixing signal at 9 GHz (lower part) vs tip bias voltage for total laser powers of 10 mW (1), 20 mW (2), 40 mW (3), and 80 mW (4). (b) Calculated mixing signals for the same laser powers as in (a).

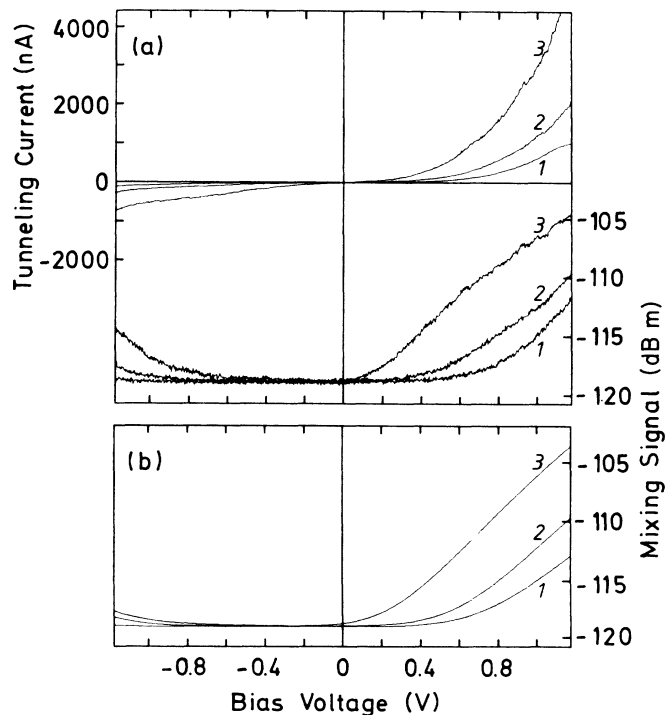


FIG. 2. (a) Plot of the tunneling current (upper part) and the mixing signal at 9 GHz (lower part) vs tip bias voltage for a total laser power of 30 mW and different tip-sample distances. (b) Calculated mixing signals for the same parameters as in (a).

less than 25% of the current and by less than 3 dB for the mixing signal. We ascribe these deviations to the following facts. During the voltage scans neither horizontal nor vertical drifts of the tip position can be excluded. In addition, at ambient air pressure fluctuations of gas molecules and adsorbates due to the high fields near the tip can affect the measurements. The I - V curves in the figures exhibit a nonlinear current rise and higher tunneling currents at positive tip polarity. The mixing-signal traces are limited to -119 dBm by the noise level which corresponds to the amplifier noise at a resolution bandwidth of the spectrum analyzer of 215 kHz.

When the laser power is increased the mixing signal rises; the I - V characteristics, however, are not significantly changed. This is shown in Fig. 1(a) for total laser powers of 10, 20, 40, and 80 mW. Beyond 100 mW, saturation of the mixing signals was observed. This was found at 9 GHz (Ref. 4) as well as below 100 MHz.⁸

Decreasing the tip-sample distance leads to an increase of the mixing signal. This has also already been observed at difference frequencies below 100 MHz.^{3,4} The results for 9 GHz are shown in Fig. 2(a), where the mixing signal and the corresponding I - V curves are plotted for different gap widths.

Finally, a dc current at zero-bias voltage was measured when the STM was illuminated with CO₂ laser radiation. For this purpose the current-feedback loop was opened, and after disconnecting the bias voltage an ammeter was connected between the tip and the surface. As an example, at 30 mW of incident laser power and a gap width determined by a tunneling current of 500 nA and a tip bias voltage of +1 V the detected current at zero-bias voltage was 660 pA. The current caused the tip to become negative.

IV. DISCUSSION

The response of the tunneling junction of the STM to laser radiation is described by using a model applied in the past to MIM point contacts.⁹ Owing to its nonlinear current-voltage characteristic the tunneling junction of the STM acts as a diode. Laser radiation is coupled into this diode by means of the tungsten tip, which represents a long-wire antenna for the infrared radiation. The oscillating antenna currents produce an alternating voltage (optical voltage) in the tunneling gap. The nonlinearity of the diode is the origin of new frequency components of the current, e.g., at zero frequency (rectification) and at the difference frequency of two injected laser signals. As before, the tip serves as an antenna now transmitting a signal at the difference frequency.

Provided the response of the junction is sufficiently fast, the static I - V characteristic can be used to calculate the new current components. The total tunneling current I can be expressed as a power series in terms of the laser-induced optical voltage V_i :

$$I = I(V_b) + (\partial I / \partial V) V_i + \frac{1}{2} (\partial^2 I / \partial V^2) V_i^2 + \dots, \quad (1)$$

where V_b is the external-bias voltage, and the derivatives are evaluated at V_b . By introducing $V_i = v_i \cos \omega_i t$ ($i = 1, 2$) into (1) it is seen that both the rectified current

and the current $I_{\Delta\omega}$ at the difference frequency $\Delta\omega = \omega_1 - \omega_2$ are proportional to the second derivative or the curvature of I at the applied-bias voltage. As the radiated power $P_{\Delta\omega}$ at the difference frequency grows as $I_{\Delta\omega}^2$, one finally obtains

$$P_{\Delta\omega}(V_b) \sim (\partial^2 I / \partial V^2)^2 P_{\omega_1} P_{\omega_2}, \quad (2)$$

where P_{ω_1} and P_{ω_2} are the laser powers at ω_1 and ω_2 .

The model was tested by comparing the measured bias dependence of $P_{\Delta\omega}$ shown in the figures with a calculation based on the experimental I - V characteristics and Eq. (2). For this purpose the averaged I - V curves shown in Figs. 1(a) and 2(a) were approximated by fifth-degree polynomials which served to calculate $\partial^2 I / \partial V^2$. Equation (2) was rewritten by using the parameters α and γ :

$$P_{\Delta\omega}(V_b) = \alpha (\partial^2 I / \partial V^2)^2 P_{\omega_1} P_{\omega_2} + \gamma. \quad (3)$$

The constant γ represents the observed noise level. The parameter α was obtained from Eq. (3) by inserting one experimental value of each mixing-signal curve shown in Figs. 1(a) and 2(a) and the corresponding value of $\partial^2 I / \partial V^2$. P_{ω_1} and P_{ω_2} were identified with the laser powers measured at the STM. Now $P_{\Delta\omega}(V_b)$ can be calculated, the resulting curves being shown in Figs. 1(b) and 2(b). In Fig. 1(b) the same value of α was used for all four traces.

Considering the spread of the unaveraged experimental traces, the agreement between the experimentally observed mixing signals and the curves calculated according to Eq. (3) is good in the two figures. In addition to the dependence of the power of the mixing signal on $(\partial^2 I / \partial V^2)^2$, Fig. 1 also demonstrates the quadratic dependence of the signals on the incident total laser power up to 80 mW. These results support the model described and its main assumption that the generation of GHz difference frequencies in the tunneling junction of the STM is predominantly determined by the nonlinearity of the static current-voltage characteristic.

From estimates of the RC time constant of the tunneling junction³ and from evidence obtained with MIM diodes it is expected that even higher frequencies can be generated in the STM. Using CO₂ laser radiation, we recently obtained difference frequencies of up to 5 THz in the STM.¹⁰ Therefore we conclude that the measured dc current at zero-bias voltage mainly results from a rectification process reaching up to the CO₂ laser line frequency of about 32 THz.

We conclude from our results that, in order to determine the fundamental physical mechanisms responsible for the mixing process in the STM, the shape of the I - V characteristic has to be studied in detail. In the usual STM theory, the geometry and the surface density of states of the tip and the sample are the most important parameters for calculating the bias-dependent tunneling current.¹¹ When electromagnetic radiation is coupled into the tunneling junction, the effects of the optical field, the enhanced temperature of the tip and the sample, and the contribution of the rectified current have to be considered. Therefore, additional mechanisms of electron transport such as photoemission, Schottky emission, or field emission may contribute to the tunneling process in the STM.

Finally, as an interesting consequence of our results, we mention that during a lateral scan, in addition to the tunneling current, also $\partial^2 I / \partial V^2$ and hence the difference-frequency signal will show variations reflecting the atomic

surface corrugation. Recently we obtained atomic-resolution images of a graphite surface, using the 9-GHz mixing signal.¹²

*Permanent address: Institute of Physical and Chemical Research, Horisawa 2-1, Wako-shi, Saitama, 351-01, Japan.

¹See, for example, L. O. Hocker, D. R. Sokoloff, V. Daneu, A. Szoke, and A. Javan, *Appl. Phys. Lett.* **12**, 401 (1968); K. J. Siemsen and H. D. Riccius, *Appl. Phys. A* **35**, 177 (1984).

²L. Arnold, W. Krieger, and H. Walther, *Appl. Phys. Lett.* **51**, 786 (1987).

³L. Arnold, W. Krieger, and H. Walther, *J. Vac. Sci. Technol. A* **6**, 466 (1988).

⁴W. Krieger, H. Koppermann, T. Suzuki, and H. Walther, *IEEE Trans. Instrum. Meas.* **IM-38**, 1019 (1989).

⁵P. H. Cutler, T. E. Feuchtwang, T. T. Tsong, H. Nguyen, and A. A. Lucas, *Phys. Rev. B* **35**, 7774 (1987).

⁶H. Q. Nguyen, P. H. Cutler, T. E. Feuchtwang, Zhi-Hong Huang, Y. Kuk, P. J. Silverman, A. A. Lucas, and T. E. Sul-

livan, *IEEE Trans. Electron Devices* **36**, 2671 (1989).

⁷T. K. Gustafson and T. J. Bridges, *Appl. Phys. Lett.* **25**, 56 (1974).

⁸H. Koppermann, Diploma thesis, Ludwig-Maximilians-Universität München, 1988.

⁹S. M. Faris, T. K. Gustafson, and J. C. Wiesner, *IEEE J. Quantum Electron.* **QE-9**, 737 (1973); A. Sanchez, C. F. Davis, Jr., K. C. Liu, and A. Javan, *J. Appl. Phys.* **49**, 5270 (1978).

¹⁰J.-P. Thost, Diploma thesis, Ludwig-Maximilians-Universität München, 1989.

¹¹J. Tersoff and D. R. Hamann, *Phys. Rev. Lett.* **50**, 1998 (1983).

¹²M. Völcker, T. Suzuki, W. Krieger, and H. Walther (unpublished).